Flattened optical frequency-locked multi-carrier generation by cascading one directly modulated laser and one phase modulator

Jianguo Yu (余建国)[1], Xinying Li (李欣颖)[2], Jianjun Yu (余建军)[2*], and Nan Chi (迟 楠)[2]

[1]*Department of Electrical Engineering, Beijing University of Posts and Telecommunications, Beijing 100876, China*

[2]*Department of Communication Science and Engineering, Fudan University, Shanghai 200433, China*

[*]*Corresponding author: jianjun@fudan.edu.cn*

Received July 11, 2013; accepted September 4, 2013; posted online November 4, 2013

We propose a novel scheme for optical frequency-locked multi-carrier generation based on a directly modulated laser (DML) and a phase modulator (PM) in cascade through synchronous sinusoidal radio frequency (RF) signal. The optimal operating zone for the cascaded DML and PM scheme is determined via theoretical analysis and numerical simulation. We demonstrate 16 optical subcarriers can be successfully generated based on the cascaded DML and PM scheme in the optimal zone. The generated 16 optical subcarries have frequency spacing of 12.5 GHz and power difference of less than 3 dB. These results agree well with those of the numerical simulation. We also demonstrate intensity modulation and direct detection (IM-DD) based on one of the 16 generated optical subcarriers. After 20-km single-mode fiber-28 (SMF-28) transmission, the bit-error ratio (BER) of 1×10^{-9} can be attained for both 3.125- and 12.5-Gb/s bit rates.

OCIS codes: 060.0060, 060.4080, 060.5060.

doi: 10.3788/COL201311.110606.

Optically coherent and frequency-locked multi-carrier generation has been intensively studied because it can offer several remarkable applications, such as wavelength -division-multiplexing (WDM) source in optical communication[1−4], reconfigurable optical pulse generator[5] and optical signal processing[6]. Several methods are used in realizing optical frequency-locked multi-carrier generation. The method based on in-phase/quadrate (I/Q) modulator combined with recirculating frequency shifter (RFS)[7−13] has the advantages of flexible control and accurate frequency spacing with lower driving voltage. However, the structures is relatively complicated. The method based on cascaded intensity modulator (IM) and phase modulator (PM) can generate multiple flattened optical subcarriers with a large tone-to-noise ratio (TNR). However, a large insertion loss (usually more than 10 dB) is observed because of the adoption of IM and the stability is also weak due to direct current (DC) bias[14,15]. We have demonstrated flattened comb generation using only PMs driven by fundamental frequency sinusoidal sources with small frequency offset[16,17]. Relative to IM or PM, directly modulated laser (DML) has the advantages of compact size, low power consumption, and easy integration[18,19].

In this letter, we propose a novel scheme for optical frequency-locked multi-carrier generation based on one DML and one PM in cascade through synchronous sinusoidal radio frequency (RF) signal. The optimal operating zone for the cascaded DML and PM scheme is determined based on theoretical analysis and numerical simulation. We demonstrate that 16 optical subcarriers with frequency spacing of 12.5 GHz and power difference less than 3 dB can be successfully generated based on the cascaded DML and PM scheme in the optimal zone. This result agrees well with that of numerical simulation. We also arrive at intensity modulation and direct detection (IM-DD) based on one of the 16 generated optical subcarriers. After 20-km single-mode fiber-28 (SMF-28) transmission, the bit-error ratio (BER) of 1×10^{-9} can be attained for both 3.125- and 12.5-Gb/s bit rates.

Sinusoidal phase modulation of a narrow-band continuous-wavelength (CW) laser can create a frequency comb with high repetition rate, tunable frequency spacing, and stable optical central frequency. As shown in Fig. 1(a), when one PM driven by a sinusoidal RF signal at f_s is used to modulate the CW lightwave at f_c, the output electrical field of the PM can be expressed as relatively complicated

$$\begin{aligned} E_{\text{out}}(t) &= E_0 \exp(\text{j}2\pi f_c t) \exp[\text{j}R\sin(2\pi f_s t)] \\ &= K \sum_{n=-\infty}^{\infty} J_n(R) \exp[\text{j}2\pi(f_c + nf_s)t], \end{aligned} \quad (1)$$

where E_0 is the amplitude of the electrical field; J_n is the first kind of Bessel function of order n; R is the

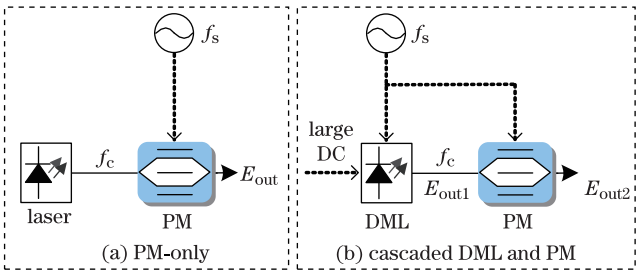

Fig. 1. Schematic diagram of comb generation based on (a) PM only and (b) cascaded DML and PM.

modulation index of the PM. The disadvantage of comb generation based only on PM is poor spectral flatness. Furthermore, the limited driving voltage of PM and the limitation of electrical amplifiers (EAs) significantly limit the modulation index of PM and the number of the generated optical subcarriers.

To overcome the disadvantages of the PM-only scheme, we propose the novel cascaded PM and DML scheme, as shown in Fig. 1(b). When biased at a large DC and driven by a sinusoidal RF signal at f_s, the output electrical field of a DML at f_c can be expressed as

$$E_{out1}(t) \approx E_0[1 + R_1 \sin(2\pi f_s t)] \exp(j2\pi f_c t), \quad (2)$$

where R_1 is the modulation index of the DML and defined by the ratio of the RF driving amplitude to the bias current for the DML. The inherent chirp from the DML is largely removed and can be neglected because of the adoption of the large DC bias[20]. Other benefits of the large bias of the DML are high output power, wide modulation bandwidth, stable single-mode operation, and low timing deviation. Thus, the output electrical field of the PM driven by the synchronous sinusoidal RF signal at f_s can be expressed as

$$\begin{aligned} E_{out2}(t) &\approx E_0[1 + R_1 \sin(2\pi f_s t)] \exp(j2\pi f_c t) \\ &\quad \exp[jR_2 \sin(2\pi f_s t)] \\ &= E_0 \sum_{n=-\infty}^{\infty} J_n(R_2) \exp[j2\pi(f_c + nf_s)t] \\ &\quad - jE_0 \frac{R_1}{2} \sum_{n=-\infty}^{\infty} J_n(R_2) \exp\{j2\pi[f_c + (n+1)f_s]t\} \\ &\quad + jE_0 \frac{R_1}{2} \sum_{n=-\infty}^{\infty} J_n(R_2) \exp\{j2\pi[f_c + (n-1)f_s]t\}, \end{aligned} \quad (3)$$

where R_2 is the modulation index of the PM and defined by the ratio of the RF driving amplitude to the half-wave voltage V_{pi} for the PM. Compared with Eq. (1), the right second and third terms of Eq. (3) can flatten the amplitude of the generated optical subcarriers spaced at f_s. Furthermore, the advantages of DML, such as low cost, compact size, and low power consumption, make the cost and integration of our proposed scheme much more efficient.

To determine the optimal operating zone for the cascaded DML and PM scheme, numerical simulation is performed based on a typical single-mode dynamic laser model (LaserSM_RE module in VPI). The laser model is based on standard rate equations and can simulate the dynamics and noise characteristics of a directly modulated single-mode laser driven by an electrical current waveform. Table 1 shows the settings for the intrinsic parameters of the laser model. The RF driving frequency f_s is 12.5 GHz, the sampling rate is 1024 GHz, and the time window is 16 ns. As indicated in the aforementioned theoretical analysis, the optimal operating zone mainly depends on the values of R_1 and R_2, as well as the laser bias current. Thus, in our simulation, the optimal operating zone is determined by sweeping the RF driving amplitude for both the laser and the PM when the laser bias current is sufficiently large.

In the absence of RF driving signal for the laser, Fig. 2 shows the calculated subcarrier number and the subcarrier power difference versus the PM driving amplitude when the laser bias current is 0.07, 0.075, and 0.08 A, respectively. The subcarrier number increases along with PM driving amplitude. The subcarrier power difference is always more than 3 dB. Therefore, optical multi-carrier generation based on phase modulation has relatively poor spectral flatness.

Figure 3 shows the variation of the calculated subcarrier number and subcarrier power difference when we simultaneously change the driving amplitude for both the laser and the PM in case of different laser bias currents (0.07, 0.075, and 0.08 A). The increase of the PM driving amplitude can enhance the subcarrier number, whereas the increase of the laser driving amplitude can not only increase the subcarrier number but also effectively decrease the subcarrier power difference. Optimal zones are marked as A, B, and C in Figs. 3(b), (d), and (f), respectively, in which the cascaded DML and PM scheme can generate 16 or more subcarriers with a power

Table 1. Intrinsic Parameters of the Laser Model

Parameters	Values	Units
Emission Frequency	193.1	THz
Reference Power	8.5	mW
Laser Chip Length	20×10^{-6}	m
Linear Material Gain Coefficient	9×10^{-20}	m^2
Transparency Carrier Density	1.5×10^{24}	m^{-3}
Confinement Factor	0.3	
Group Effective Index	4.0	
Material Linewidth Enhancement Factor	3.5	
Left Facet Reflectivity	0.3	
Right Facet Reflectivity	0.3	
Carrier Lifetime	2.1×10^{-9}	s
Spontaneous Emission Factor	1.0×10^{-4}	
Nonlinear Gain Coefficient	3.0×10^{-23}	

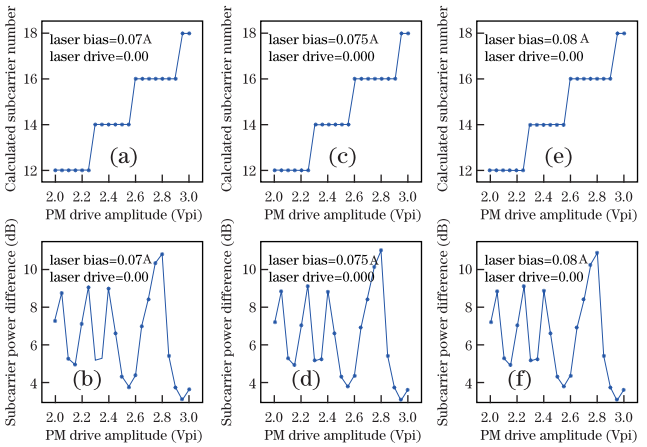

Fig. 2. Calculated subcarrier number and subcarrier power difference versus the PM driving amplitude without laser driving signal.

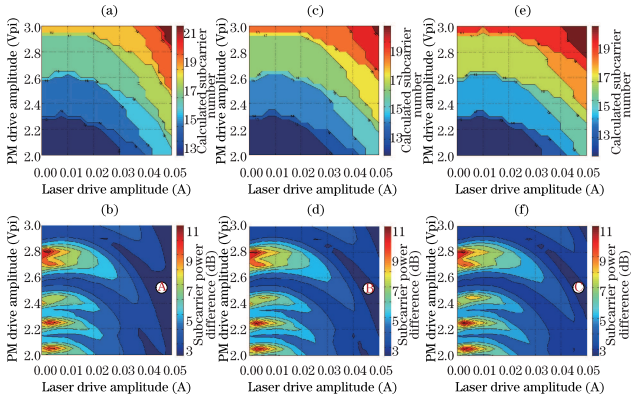

Fig. 3. Variation of calculated subcarrier number and subcarrier power difference when the driving amplitude is simultaneously changed for both the laser and the PM. (a) and (b): bias=0.07A; (c) and (d): bias=0.075A; (e) and (f): bias=0.08A.

difference of less than 3 dB. When the laser driving amplitude is further increased near the laser bias current, additional subcarriers with better spectral flatness can be generated, but with lower TNR.

When the laser bias current is 0.075 A and the PM driving amplitude is 2.4 $V_{\rm pi}$, the calculated subcarrier number and subcarrier power difference versus the laser driving amplitude are shown in Figs. 4(a) and (b). The increase of the laser driving amplitude can enhance the subcarrier number and the subcarrier spectral flatness. When the laser bias current is 0.075 A, the PM and the laser driving amplitudes are 2.4 $V_{\rm pi}$ and 0.05 A, respectively. Figures 4(c) and (d) show the calculated optical spectra of the laser and the PM, respectively. The optical spectrum of the laser is asymmetrical because of the residual chirp. Seventeen optical subcarriers exhibit a power difference of 2.56 dB after the PM.

Figure 5 shows the experimental setup for the flattened optical multi-carrier generation and linewidth measurement based on the cascaded DML and PM scheme. For optical multi-carrier generation, a 12.5-GHz sinusoidal RF signal is equally divided into two branches by a power divider. Next, one branch is power amplified to 24 dBm and used to drive the DML, whereas the other is power amplified to 30-dBm and used to drive the PM. The DML is a commercially available distributed-feedback (DFB) laser containing 74-mA DC bias and 9.3-dBm average output power. The half-wave voltage $V_{\rm pi}$ of the PM at 12.5 GHz is 4.2 V and the RF driving amplitude for the PM is approximately 10 V when the input resistance of the PM is 50 ohms. Thus, the modulation index R_2 is 2.4. The phase shifter (PS) before the PM is used to synchronize the two branches. The polarization-maintaining erbium-doped fiber amplifier (EDFA) between the cascaded DML and PM is used to compensate for the modulation loss. The subsequent polarization-maintaining tunable optical filter (TOF) with tunable bandwidth and wavelength is used to suppress the amplified spontaneous emission (ASE) noise from the polarization-maintaining EDFA. The 12.5/25-GHz optical inter-leaver (IL) together with the polarization-maintaining TOF with tunable bandwidth from 0.1 to 9 nm is used to choose the desired optical subcarrier from the generated multiple optical subcarriers. After power has been amplified by an EDFA, the selected optical subcarrier with 25-GHz bandwidth is sent into the linewidth measurement system. This system includes two polarization-maintaining optical couplers (OCs), a high-speed photo detector (PD), and a spectral analyzer.

Figure 6(a) shows the output optical power versus the input current for the DML. The threshold current of the DML is almost 15 mA. Figure 6(b) shows the output optical spectrum (0.01-nm resolution) of the DML without driving signal. The side mode suppression ratio (SMSR) of the DML is more than 40 dB. Figure 6(c) shows the output optical spectrum (0.01-nm resolution) of the DML with 24-dBm driving signal. The optical spectrum is asymmetrical at 1537.7-nm central wavelength because of the inherent chirp from the DML[18]. Figure 7(a) shows the optical spectrum (0.02-nm resolution) after the PM when the DML is without driving signal. The power difference is approximately 8 dB for 12 subcarriers, which is similar to that shown in Fig. 2. With 24-dBm laser driving signal, Figs. 7(b) and (c) show the optical spectra (0.01-nm resolution) after the PM and TOF with 3-dB bandwidth of ~1.7 nm, respectively. Accordingly, 16 optical subcarriers with 12.5-GHz frequency spacing are generated with a power difference of less than 3 dB, which agrees with and demonstrates the theoretical analysis and numerical simulation.

Figure 8(a) shows the optical spectrum (0.01-nm resolution) of the selected optical subcarrier by the TOF with 3-dB bandwidth of 0.1-nm and 12.5/25-GHz optical IL. Figure 8(b) illustrates the output electrical spectrum (300-kHz resolution) of the spectral analyzer when the

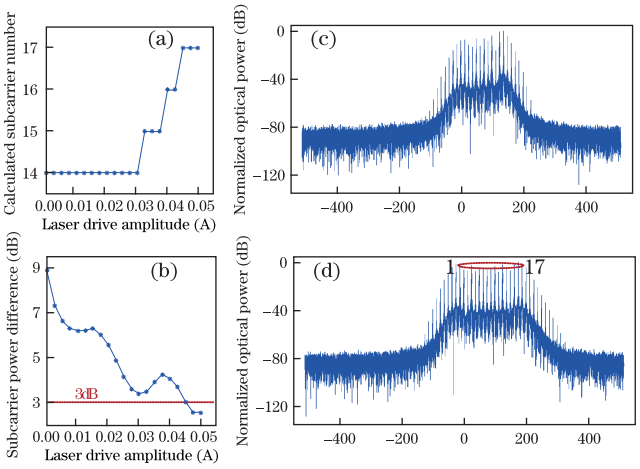

Fig. 4. (a) Calculated subcarrier number and (b) subcarrier power difference versus the laser driving amplitude; calculated optical spectra of (c) the laser and (d) the PM.

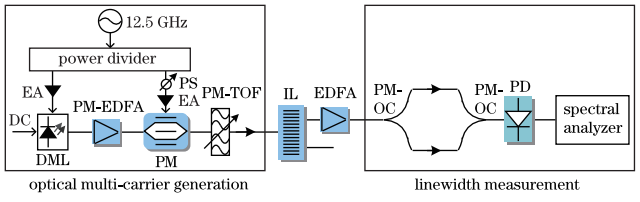

Fig. 5. Experimental setup for optical multi-carrier generation and linewidth measurement.

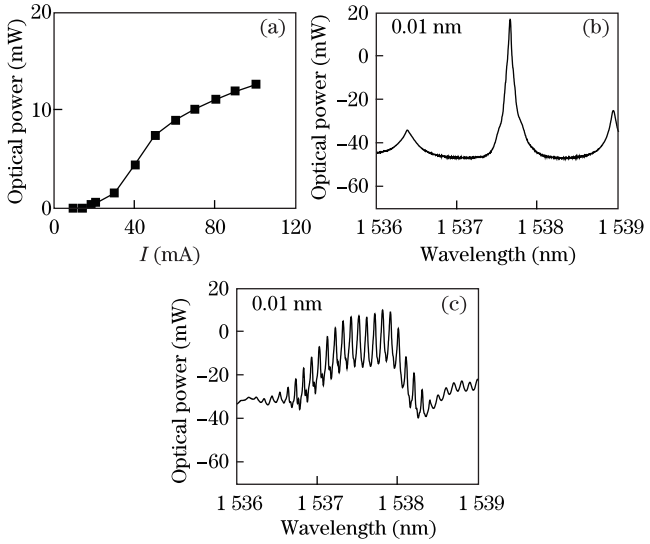

Fig. 6. (a) Output optical power versus input current for the DML. Optical spectra (0.01 nm resolution) (b) without and (c) with RF driving signal.

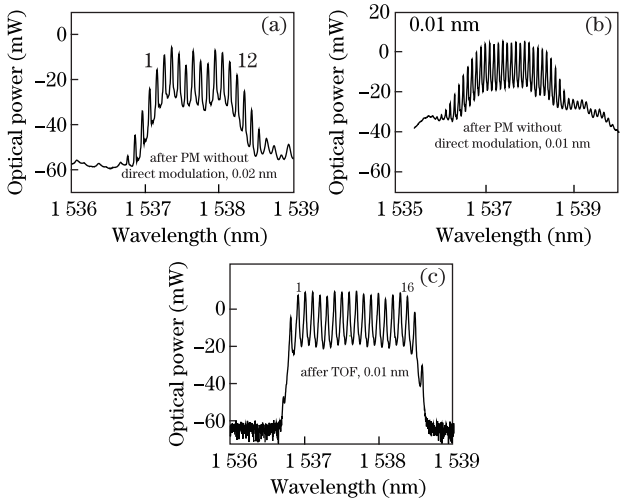

Fig. 7. Optical spectra. (a) After PM without direct modulation (0.02-nm resolution); (b) after PM with direct modulation (0.01-nm resolution); (c) after TOF (0.01-nm resolution).

selected optical subcarrier by the TOF with 3-dB bandwidth of 0.1-nm and 12.5/25-GHz optical IL is sent into the linewidth measurement system. The linewidth of the selected optical subcarrier is almost 25 MHz. After measurement, we confirm that the linewidth of the CW lightwave directly generated from the DML is also 25 MHz. Therefore, the linewidth of the generated subcarrier is not increased. The DML has short laser chip length for large modulation bandwidth, so the linewidth of the DML is wide.

Figure 9 shows the experimental setup for the flattened optical multi-carrier generation and IM-DD demonstration based on the cascaded DML and PM scheme. The optical multi-carrier generation is identical to that shown in Fig. 5. The selected optical subcarrier by the TOF with 3-dB bandwidth of 0.1-nm and 12.5/25-GHz optical IL is modulated by an IM. The IM is driven by a 12.5/3.125-Gb/s electrical binary signal, which is generated from the pulse pattern generator (PPG) with a pseudo-random binary sequence (PRBS) length of $2^{23}-1$[21]. After 20-km SMF-28 transmission, the optical signal is directly detected by a PIN receiver with 3-dB bandwidth of 7.5 GHz. The power launched into the fiber is 4 dBm. Figure 9(a) shows the optical spectrum (0.01-nm resolution) after the IM. Figures 9(b) and (c) show the eye diagrams (20 ps/div) after the PM and the second EDFA with 55-GHz oscilloscope (OSC) bandwidth, respectively. The pulsewidth from the DML laser after modulation is approximately 15 ps. Figures 9(d) and (e) show the eye diagrams (20-GHz OSC bandwidth, 100 ps/div) for the detected 3.125-Gb/s signal without and with 20-km SMF-28 transmission, respectively. Figures 9(f) and (g) show the eye diagrams (20-GHz OSC bandwidth, 20 ps/div) for the detected 12.5-Gb/s signal without and with 20-km SMF-28 transmission, respectively. The extinction ratio before transmission is more than 10 dB for both 3.125-and 12.5-Gb/s bit rates. The eye diagram amplitude after transmission is smaller than that without transmission for both 3.125-and 12.5-Gb/s bit rates. This difference is due to the lack of pre-EDFA at the receiver side and the reduced optical power after transmission.

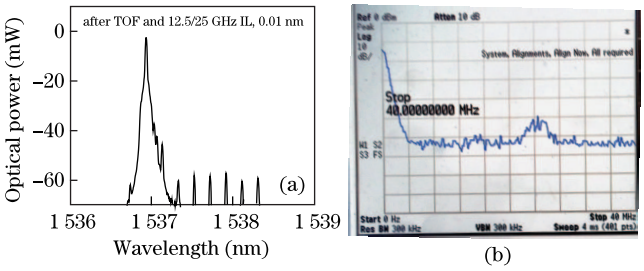

Fig. 8. (a) Optical spectrum after TOF with 3-dB bandwidth of 0.1-nm and 12.5/25 GHz IL. (b) Output electrical spectrum (300-kHz resolution) of the spectral analyzer.

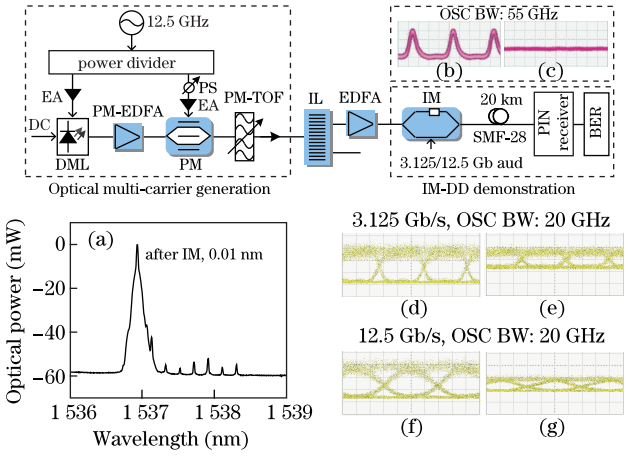

Fig. 9. Experimental setup for optical multi-carrier generation and IM-DD demonstration. (a) Optical spectrum (0.01-nm resolution) after the IM; eye diagrams (55-GHz OSC bandwidth, 20 ps/div) after (b) the PM and (c) the second EDFA; eye diagrams (20-GHz OSC bandwidth, 100 ps/div) for the detected 3.125-Gb/s signal (d) without and (e) with 20-km SMF-28 transmission; eye diagrams (20-GHz OSC bandwidth, 20 ps/div) for the detected 12.5-Gb/s signal (f) without and (g) with 20-km SMF-28 transmission.

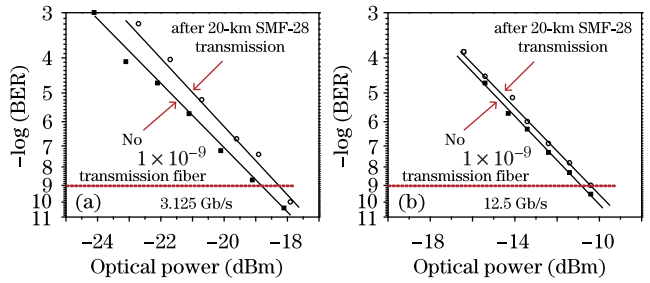

Fig. 10. Measured BER versus the optical power launched into the PIN receiver. (a) 3.125 and (b) 12.5 Gb/s.

Figures 10(a) and (b) show the measured BER versus the optical power launched into the PIN receiver for 3.125- and 12.5-Gb/s bit rates, respectively. The BER of 1×10^{-9} can be attained. The optical power penalty of almost 0.5 dB because of 20-km SMF-28 transmission can be discounted for both 3.125- and 12.5-Gb/s bit rates. At the BER of 1×10^{-9}, the required optical power for the 12.5-Gb signal is almost 8-dB larger than that for the 3.125-Gb/s signal. Theoretically, the difference should be only 6 dB. A penalty of approximately 2 dB is charged for the detection of the 12.5-Gb/s signal because the PIN receiver with 3-dB bandwidth of 7.5 GHz is designed for 10-Gb/s signal. After measurement, we confirm that all the other generated optical subcarriers perform similarly. Therefore, our proposed cascaded DML and PM scheme for optical multi-carrier generation is feasible.

In conclusion, we propose a novel scheme for optical frequency-locked multi-carrier generation based on one DML and one PM in cascade through synchronous sinusoidal RF signal. The optimal operating zone for the cascaded DML and PM scheme is determined via theoretical analysis and numerical simulation. We demonstrate 16 optical subcarriers can be successfully generated based on the cascaded DML and PM scheme in the optimal zone. The generated 16 optical subcarries have frequency spacing of 12.5 GHz and power difference of less than 3 dB. This result agrees well with the numerical simulation. IM-DD demonstration is also performed based on one of the 16 generated optical subcarriers. After 20-km SMF-28 transmission, the BER of 1×10^{-9} can be attained for both 3.125- and 12.5-Gb/s bit rates. This result demonstrates the feasibility of the cascaded DML and PM scheme for optical multi-carrier generation.

This work was supported by the National Natural Science Foundation of China (Nos. 61107064, 61177071, 60837004, and 61250018), the National High Technology Research and Development Program of China (Nos. 2011AA010302 and 2012AA011302), the National Key Technology R&D Program of China (No. 2012BAH18B00), and the International Coorperation Program of Shanghai Scvence and Technology Association (No. 12510705600).

References

1. Z. Jiang, C. Huang, D. Leaird, and A. M. Weiner, Nat. Photon. **1,** 463 (2007).
2. F. Tian, X. Zhang, J. Li, and L. Xi, J. Lightwave Technol. **29,** 1085 (2011).
3. C. Chen, C. Zhang, D. Liu, K. Qiu, and S. Liu, Opt. Lett. **37,** 3954 (2012).
4. J. Yu, Z. Dong, and N. Chi, IEEE Photon. Technol. Lett. **23,** 1061 (2011).
5. A. Clarke, D. Williams, M. Roelens, and B. Eggleton, IEEE Photon. Technol. Lett. **28,** 97 (2010).
6. P. J. Delfyett, I. Ozdur, N. Hoghooghi, M. Akbulut, J. Davila-Rodriguez, and S. Bhooplapur, IEEE J. Sel. Top. Quantum Electron. **18,** 258 (2012).
7. J. Li, X. Li, X. Zhang, F. Tian, and L. Xi, Opt. Express **18,** 17597 (2010).
8. J. Zhang, J. Yu, N. Chi, Z. Dong, X. Li, Y. Shao, and L. Tao, Opt. Lett. **37,** 4714 (2012).
9. X. Li, J. Yu, Z. Dong, J. Zhang, Y. Shao, and N. Chi, Opt. Express **20,** 21833 (2012).
10. J. Li and Z. Li, Opt. Lett. **38,** 359 (2013).
11. J. Zhang, J. Yu, N. Chi, Y. Shao, L. Tao, J. Zhu, and Y. Wang, J. Lightwave Technol. **30,** 3938 (2012).
12. J. Zhang, J. Yu, N. Chi, Y. Shao, L. Tao, Y. Wang, and X. Li, IEEE Photon. Technol. Lett. **24,** 1405 (2012).
13. J. Yu, Z. Dong, J. Zhang, X. Xiao, H. C. Chien, and N. Chi, J. Lighwave Technol. **30,** 458 (2012).
14. Y. Dou, H. Zhang, and M. Yao, Opt. Lett. **36,** 2749 (2011).
15. S. Zou, Y. Wang, Y. Shao, J. Zhang, J. Yu, and N. Chi, Chin. Opt. Lett. **10,** 070605 (2012).
16. J. Zhang, J. Yu, L. Tao, Y. Fang, Y. Wang, Y. Shao, and N. Chi, J. Lightwave Technol. **30,** 3911 (2012).
17. J. Zhang, J. Yu, N. Chi, Z. Dong, X. Li, Y. Shao, J. Yu, and L. Tao, Opt. Lett. **38,** 552 (2013).
18. H. Hu, J. Yu, L. Zhang, A. Zhang, Y. Li, Y. Jiang, and E. Yang, Opt. Express **15,** 8931 (2007).
19. J. Yu, Z. Jia, M. Huang, M. Haris, P. Ji, T. Wang, and G. Chang, J. Lightwave Technol. **27,** 253 (2009).
20. D. Mahgerefteh, Y. Matsui, X. Zheng, and K. McCallion, IEEE J. Sel. Top. Quantum. Electron. **16,** 1126 (2010).
21. C. Tang, R. Li, Y. Shao, N. Chi, J. Yu, Z. Dong, and G. Chang, Chin. Opt. Lett. **11,** 020608 (2013).